Measurement selection for on-line estimation of nonlinear wave models for high purity distillation columns

Shoujun Bian, Michael A. Henson*

Department of Chemical Engineering, University of Massachusetts, Amherst, MA 01003-9303, USA

Abstract

Nonlinear wave models are commonly used to provide a reduced-order description of distillation column dynamics. Due to the simplified model structure, on-line parameter estimation is typically required for satisfactory prediction of column performance. In this paper an approach for selecting stage composition/temperature measurements for on-line estimation of wave model parameters is presented. We focus on high purity distillation columns which are particularly challenging due to the presence of highly pinched composition profiles. The proposed method provides a compromise between two competing effects, the sensitivity of stage composition predictions to model parameters and collinearities between these sensitivities. An iterative calculation procedure based on a scaled sensitivity matrix yields a ranking of the stage compositions according to their usefulness for parameter estimation. Two high purity column simulators are used to illustrate the measurement selection procedure and the subsequent design of nonlinear state/parameter estimators using the extended Kalman filtering approach. The proposed method is shown to be more flexible than a conventional measurement selection technique based on singular value decomposition.
© 2005 Elsevier Ltd. All rights reserved.

Keywords: High purity distillation column; Nonlinear wave model; Measurement selection; State and parameter estimation

1. Introduction

Control system design for high purity distillation columns is inherently difficult due to nonlinear process dynamics and the complexity of rigorous column models. Although other nonlinear controller design strategies have been proposed, nonlinear model predictive control (NMPC) appears to be the most promising technology for nonlinear processes such as distillation columns characterized by multivariable interactions and operational constraints (Henson, 1998; Mayne et al., 2000). The NMPC approach requires repeated on-line solution of an open-loop optimal control problem over a prediction horizon into the future. An objective function involving the deviation of predicted controlled outputs from their setpoint values is minimized by treating the manipulated inputs as decision variables. Simultaneous solution methods involve temporal discretization of the model equations to yield a large set of nonlinear algebraic equations which are posed as constraints in a

nonlinear programming problem (Biegler et al., 2002; Meadows and Rawlings, 1997). The computational difficulty of the NMPC problem is intimately connected with the complexity of the controller design model.

Rigorous distillation column models are comprised of nonlinear differential and algebraic equations involving stage compositions, temperatures and holdups. Due to their high dimensionality, these models are difficult to incorporate within NMPC controllers. A promising sequential solution strategy based on specialized multiple shooting and reduced successive quadratic programming techniques has been successfully applied to a distillation column of moderate complexity (Nagy et al., 2000). However, there is clear motivation to develop simpler nonlinear models that capture the essential column dynamics. A popular approach is nonlinear wave modeling where the high order column dynamics are reduced to a single differential equation for the traveling composition or temperature wave in each column section (Gilles and Retzbach, 1983; Hwang, 1987; Hwang and Helfferich, 1988; Luyben, 1972; Marquardt, 1986; Zhu et al., 2001). A dramatic reduction in model dimensionality is achieved by exploiting the traveling wave nature of column

---

* Corresponding author. Tel.: +1 413 545 3481; fax: +1 413 545 1647.
 E-mail address: henson@ecs.umass.edu (M.A. Henson).

profiles and through the introduction of several simplifying assumptions such as a binary mixture, ideal vapor–liquid equilibrium, equimolar overflow and constant holdups.

A common problem observed with nonlinear wave models is that they are incapable of generating accurate predictions over a wide range of operating conditions due to these simplifying assumptions. Several investigators have proposed nonlinear parameter estimation as a means to improve wave model predictions (Balasubramhanya and Doyle, 1997; Bian et al., 2005; Rehm and Allgower, 1996). Stage composition and/or temperature measurements are used to generate on-line estimates of key wave model parameters and the unmeasured wave position. An important consideration is the selection of appropriate measurement locations for this on-line state and parameter estimation problem. Measurement selection is particularly critical for high purity columns with highly pinched profiles. Measurements located within pinched regions do not provide useful information for wave parameter estimation because they are insensitive to changes in profile position and shape.

General measurement selection techniques based on singular value decomposition (SVD) (Oisiovici and Cruz, 2001) and various information theoretic and data reconciliation metrics (Bagajewicz, 1997; Chmielewski et al., 2002; Muske and Georgakis, 2003) have been proposed. Limitations of SVD based methods include: (1) the number of selected measurements must equal the number of estimated variables; and (2) the algorithm is not designed to allow a priori inclusion of preselected measurements. The first limitation is particularly important for high purity columns where additional stage composition measurements may be needed to account for the movement of pinched regions resulting from changes in column operating conditions. The second limitation is relevant for columns which have preexisting measurements that must be incorporated within the estimator design. The contribution of this paper is the development and evaluation of a measurement selection technique that can be viewed as an extension of SVD based methods in the sense that these two limitations are removed. While this paper focuses entirely on the problem of measurement selection for state and parameter estimation in nonlinear wave models, the proposed method is generally applicable.

The remainder of this paper is organized as follows. A brief overview of the nonlinear wave modeling approach is presented in Section 2. The proposed measurement selection procedure is described in Section 3. Application of the proposed method is illustrated using a nitrogen purification column (Section 4) and a benzene–toluene separation column (Section 5). A summary and conclusions are provided in Section 6.

2. Nonlinear wave modeling

The distillation column is divided into sections according to the location of feed and side withdrawal streams. Each section is described by a single differential equation for the wave position and nonlinear algebraic equations that allow reconstruction of the binary liquid and vapor composition profiles from the wave position. The wave position equation is obtained via material balance across the shock wave (Marquardt, 1986)

$$w = \frac{\mathrm{d}s}{\mathrm{d}t} = \frac{1}{N_t} \frac{-L(x_{in} - x_{out}) + V(y_{out} - y_{in})}{n_l(x_{in} - x_{out}) + n_v(y_{out} - y_{in})}, \quad (1)$$

where s is the wave position which represents the inflection point the wave profile; L and V are internal liquid and vapor molar flow rates, respectively; N_t is the total number of equilibrium stages in the column section; n_l and n_v are the liquid and vapor molar holdups, respectively, of a single stage; x_{in} and x_{out} are the compositions of the liquid streams entering and exiting, respectively, the column section; and y_{in} and y_{out} are corresponding compositions of the liquid streams.

The vapor and liquid composition profiles are calculated from the wave position s and the relative volatility α as

$$y(z) = y_{min} + \frac{y_{max} - y_{min}}{1 + \exp[\gamma(z - s)]}, \quad (2)$$

$$x(z) = \frac{y(z)}{\alpha - (\alpha - 1)y(z)}, \quad (3)$$

where z is dimensionless position inside the column section (0 is the bottom and 1 is the top); γ is the wave front slope; y_{max} and y_{min} are the upper and lower asymptotical limits, respectively, of the wave profile. The composition of the exiting vapor stream y_{out} is calculated from (2) with $z = 1$. The exiting liquid composition x_{out} is calculated from (2) with $z = 0$ and (3). The entering compositions y_{in} and x_{in} are determined from material balances on the feed/withdrawal stages, condenser and/or reboiler that delimit the column section. Therefore, the complete wave model consists of the wave position equation (1) and the composition profile equations (2) and (3) written for each column section combined with mass balances for feed/withdrawal stages, condenser and reboiler. This compact representation is the major motivation for using nonlinear wave models as the basis for nonlinear controller design.

The wave model parameters γ, y_{max} and y_{min} that determine the composition profile shape can be estimated off-line from steady-state composition data (Zhu et al., 2001). These parameters are truly constants only for idealized columns of infinite length (Marquardt, 1986). For real columns with non-ideal behavior, the wave model parameters must be adjusted to provide satisfactory predictions over a range of steady-state operating points. Several investigators have proposed on-line state and parameter estimation as a means to improve wave model accuracy (Balasubramhanya and Doyle, 1997; Bian et al., 2005; Rehm and Allgower, 1996). The first step is to select a set of composition/temperature measurements that provide sufficient information on the composition profile behavior. In the next section, we propose a general and systematic procedure for selecting potential measurements for combined state and parameter estimation.

3. Measurement selection procedure

The success of nonlinear state and parameter estimation strategies is critically dependent on the availability of measurements that adequately characterize process behavior. For

nonlinear wave models of distillation columns the problem involves the selection of stage composition and/or temperature measurements that provide information on the composition profile. Many columns have existing measurements that should be utilized to reduce the cost of adding new stream sampling and composition analysis systems. The measurement selection problem is particularly challenging for high purity columns because: (1) the composition profile may be highly pinched such that measurements located in the pinched region provide no useful information; and (2) the location of the pinched region can move dramatically in response to changes in column operating conditions. Poorly selected measurement locations can lead to unsatisfactory performance or even divergence of the combined state/parameter estimator (Bian et al., 2005).

Measurement selection techniques are usually based on the sensitivity matrix between the estimated parameters and the candidate measurements. Many methods involve decomposition of the sensitivity matrix into principal components using SVD (Luyben, 1973; Oisiovici and Cruz, 2001). The largest element of each principal component is used to a identify a single measurement, thereby yielding a measurement vector with dimension equal to the number of estimated variables. For high purity columns such as those studied in this paper, we have shown that additional measurements may be needed to successfully estimate wave model parameters over a wide range of feed rates (Bian et al., 2005). Furthermore, SVD methods are not designed to allow a priori inclusion of existing measurements. Below we present a general measurement selection procedure that overcomes the limitations of existing SVD based techniques.

The proposed method is based on the scaled sensitivity matrix between the estimated variables and the candidate measurements. For nonlinear wave models the estimated variables are the unmeasured wave positions and wave model parameters while the candidate measurements are stage compositions. Although not considered in this paper, the selected stage compositions can be replaced with pressure corrected temperature measurements to facilitate practical implementation (Bian et al., 2005). The elements of the scaled sensitivity matrix are defined as

$$K_{ij} = \frac{\partial y_i / \bar{y}_i}{\partial p_j / \bar{p}_j}, \tag{4}$$

where p is the vector of estimated variables, y is the vector of candidate measurements, and $\bar{p}$ and $\bar{y}$ are nominal values corresponding to a particular steady-state operating point. A large sensitivity coefficient K_{ij} indicates that the output y_i provides useful information for estimation of the variable p_j. The nonlinear wave model equations can be represented as

$$\frac{\mathrm{d}s}{\mathrm{d}t} = f(s, \theta), \tag{5}$$

$$y = g(s, \theta), \tag{6}$$

where s is the vector of wave positions and θ is the vector of wave model parameters. The partial derivatives required to calculate the sensitivity matrix are

$$\frac{\partial y}{\partial s} = \frac{\partial g(s, \theta)}{\partial s}, \tag{7}$$

$$\frac{\partial y}{\partial \theta} = \frac{\partial g(s, \theta)}{\partial s} \frac{\partial s}{\partial \theta} + \frac{\partial g(s, \theta)}{\partial \theta}. \tag{8}$$

The partial derivatives with respect to s can be computed analytically as shown. Because an explicit relationship $s = h(\theta)$ cannot be constructed, the partial derivatives with respect to θ are computed numerically using finite differences by introducing 1% changes in the model parameters.

The proposed measurement selection method yields a ranking of the candidate measurements according to their usefulness for combined state/parameter estimation. The technique involves the calculation of two competing measures: (1) the overall sensitivity of a candidate measurement to changes in the estimated variables; and (2) the uniqueness of these parameter effects as reflected by the sensitivity vectors. An iterative calculation procedure is used to achieve a suitable tradeoff between the two measures and produce the ranking of candidate measurements. We have previously utilized the selection method in the development of an output feedback control strategy for the nitrogen purification column considered in this paper (Bian et al., 2005).

The iterative algorithm described as follows is an extension of a parameter selection procedure recently developed by our group (Li et al., 2004):

1. Calculate the scaled sensitivity matrix $K = \{K_{ij} = (\partial y_i / \bar{y}_i)/(\partial p_j / \bar{p}_j)\}$ where p_j, $j \in [1, q]$, is the jth estimated variable and y_i, $i \in [1, m]$, is the ith candidate measurement.

2. Perform principal component analysis (PCA) (Dunteman, 1989) on the covariance matrix: $X = K^{\mathrm{T}}K \in R^{m \times m}$. Denote λ_i as the ith eigenvalue of X and c_{ji} as the jth element of the ith principle component. The weighted sum of the principle component elements and their corresponding eigenvalues

$$E_j = \frac{\sum_{i=1}^{m} |\lambda_i c_{ji}|}{\sum_{i=1}^{m} |\lambda_i|} \in [0, 1] \tag{9}$$

is a measure of the overall response of the jth measurement to variations in the estimated variables. Select the candidate measurement with the largest E_j value as the first measurement.

3. For the second to qth measurements, determine the smallest distance vector in the space spanned by the sensitivity vectors of the n measurements already chosen. Assume the sensitivity vectors $s_k = [K_{k1} \ K_{k2} \ \cdots \ K_{kq}]^{\mathrm{T}}$ are linearly independent for $k \in [1, n]$ where $1 \leqslant n < q$. Otherwise, the sensitivity vectors of the remaining measurements are necessarily linearly dependent with the sensitivity vectors of the measurements already chosen and the algorithm must be terminated. Any vector $\bar{s}$ in the n-dimensional vector space
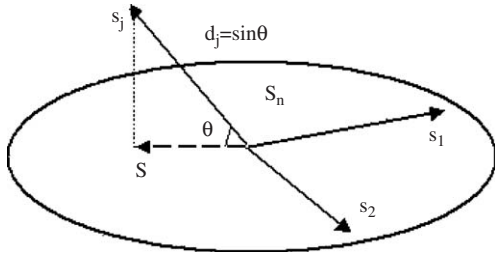
Fig. 1. Determination of the collinearity measure.

S_n can be expressed as

$$\bar{s} = \sum_{k=1}^{n} a_k s_k, \tag{10}$$

where the a_k are constants. Consider the sensitivity vector s_j associated with a candidate measurement not already selected. The vector closest to s_j in the space S_n is determined as

$$\min_{a_k} \frac{1}{2}(s_j - \bar{s})^{\mathrm{T}}(s_j - \bar{s}). \tag{11}$$

The determination of the minimum distance vector is illustrated in Fig. 1 for the simple case where two measurements with sensitivity vectors s_1 and s_2 have already been chosen. Compute the following measure $d_j \in [0, 1]$ that quantifies the degree of collinearity between the candidate sensitivity vector s_j and the minimum distance sensitivity vector $\bar{s}$:

$$d_j = \sin\left[\cos^{-1}\left(\frac{s_j^{\mathrm{T}}\bar{s}}{\|s_j\| \cdot \|\bar{s}\|}\right)\right], \tag{12}$$

where $\|\cdot\|$ represents the Euclidean norm. Measurements with large d_j values are favored for selection because they provide unique information compared to the measurements already chosen. Calculate the identifiability indices $I_j = E_j d_j \in [0, 1]$. Select the candidate measurement with the largest I_j value as the next measurement.
4. For the $(q+1)$th to mth measurements, form all possible $(p-1)$-tuples of the previously selected measurements. The number of possible combinations is

$$r = \frac{k!}{(q-1)!(k-q+1)!}, \quad q+1 \leqslant k \leqslant m. \tag{13}$$

Use (12) to compute the linear independence metric $d_{r,j}$ with respect to the j candidate measurements for all r possible combinations. Determine the worst case over all possible combinations: $d_j = \min_r d_{r,j}$. Calculate the identifiability index I_j for each candidate measurement. Select the candidate measurement with the largest I_j value as the next measurement. Terminate the algorithm when all the measurements have been selected.

This iterative algorithm yields a ranking of all candidate measurements according to their expected information content. As shown below for two high purity distillation columns, the actual

number of measurements needed for successful state and parameter estimation must be determined by simulation study. We have found that robust estimator performance can be achieved over a range of column operating conditions with only one more measurement than the number of estimated variables. Therefore, the selection algorithm can be terminated soon after the number of ranked measurement exceeds the number of estimated variables. This simplification allows the possible combinatorial explosion of measurement combinations in step 4 to be avoided.

An inherent limitation of the proposed method is that measurement selection is based entirely on the steady-state sensitivity matrix. The shortcomings of this approach include: (1) the actual information content of the candidate measurements under typical operating conditions is not considered; (2) the measurement rankings obtained are local and dependent on the steady state chosen as the base case; and (3) dynamic and nonlinear effects are neglected. In the case studies presented below, we indirectly address the nonlinearity problem by utilizing a composite sensitivity matrix obtained by averaging over several steady states. While other extensions are possible, the remainder of this paper is focused on evaluating the effectiveness of the basic measurement selection strategy described above.

4. Nitrogen purification column

4.1. Model formulation

The nitrogen purification column is the simplest distillation column in a typical cryogenic air separation plant (Isalski, 1989). A liquid distributor is placed in the middle of the packed column to improve the flow characteristics of the descending liquid. A reboiler is not necessary because an air feed stream with a high vapor fraction is introduced to the bottom of the column. The liquid level in the bottoms sump is controlled by adjusting the bottoms liquid flow rate. The overhead vapor is split into the vapor nitrogen product and a stream introduced to a total condenser. Most of the condensate is returned to the column as reflux with only a small portion withdrawn as the liquid nitrogen product. The liquid level in the reflux drum is controlled using the reflux flow rate. A detailed simulation of the nitrogen purification column was built in Aspen Dynamics with thermodynamic data for the ternary mixture of nitrogen, oxygen and argon provided by Praxair. The simulator was employed as a surrogate plant in our on-line estimation studies. The nominal column operating conditions used are shown in Table 1. Four other steady states corresponding to feed flow rate changes of ± 5 kmol/h and ± 10 kmol/h from the nominal value were investigated to cover a reasonably large range of operating conditions.

Because the nitrogen column only contains a rectifying section, a single wave equation is sufficient to model the column dynamics. Several assumptions were invoked to simplify wave model construction: (1) air can be treated as a pseudo-binary mixture with nitrogen and argon lumped into a single component with the thermodynamic properties of nitrogen; and (2) the dynamics of the feed stage, liquid distributor and condenser

Table 1
Nominal operating conditions for nitrogen purification column

Variable	Symbol (units)	Value
Feed flow rate	F (kmol/h)	98.4
Feed vapor fraction	q (kmol/kmol)	0.963
Feed O_2 composition	z_f (kmol/kmol)	0.2096
Top stage vapor composition	y_{out} (ppm)	2.81
Average liquid holdup on each stage	n_l (kmol)	0.0852
Average vapor holdup on each stage	n_v (kmol)	0.0186
Liquid product flow rate	$LN2$ (kmol/h)	0.117
Vapor product flow rate	$GN2$ (kmol/h)	49.134
Reflux flow rate	L (kmol/h)	45.508

Table 2
Measurement selection results for the nitrogen purification column

Method	Steady-state	1st	2nd	3rd	4th	5th	6th
PCA	Nominal	1	32	40	25	36	15
PCA	$F - 5\,\text{kmol/h}$	3	9	1	6	11	41
PCA	$F - 10\,\text{kmol/h}$	1	7	4	2	5	8
PCA	$F + 5\,\text{kmol/h}$	33	1	40	37	21	39
PCA	$F + 10\,\text{kmol/h}$	30	38	40	1	21	35
PCA	Averaged gain	1	33	12	40	3	41
SVD	Nominal	1	32	41	N/A	N/A	N/A
SVD	$F - 5\,\text{kmol/h}$	3	9	1	N/A	N/A	N/A
SVD	$F - 10\,\text{kmol/h}$	1	7	4	N/A	N/A	N/A
SVD	$F + 5\,\text{kmol/h}$	33	1	41	N/A	N/A	N/A
SVD	$F + 10\,\text{kmol/h}$	30	38	41	N/A	N/A	N/A
SVD	Averaged gain	1	33	12	N/A	N/A	N/A
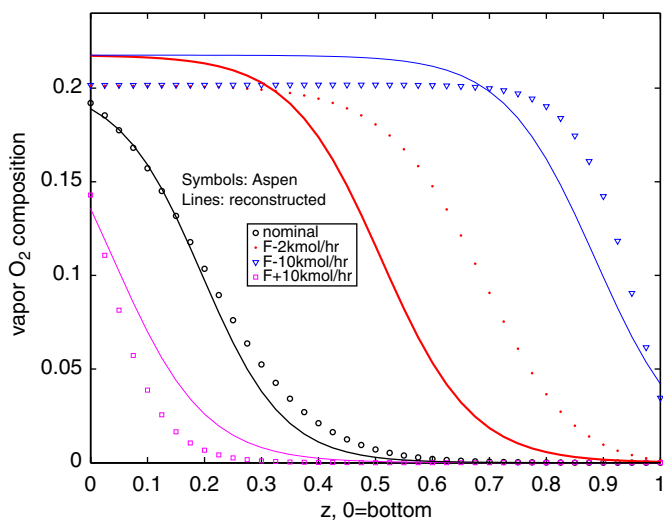
Fig. 2. Open-loop simulation results for the nitrogen purification column.

are negligible compared to the column dynamics. The large liquid holdup of the distributor was divided equally between the 41 equilibrium stages. The resulting wave model consists of a single nonlinear differential equation for the wave position and six nonlinear algebraic equations for the feed stage, total condenser and vapor–liquid equilibrium relations. Additional details on the formulation of the nonlinear wave model are provided in our previous publications (Bian et al., 2005; Zhu et al., 2001). Nominal values of the wave parameters were regressed using least-squares estimation

$$\min_{s, \gamma, y_{max}, y_{min}} \sum_{i=1}^{N_t} [y_p(z_i) - \hat{y}(z_i)]^2, \qquad (14)$$

where z_i is the dimensionless column position with 0 being the bottom and 1 being the top; N_t is the number of data points; $y_p(z_i)$ is the vapor composition obtained from the Aspen simulator; and $\hat{y}(z_i)$ is the predicted vapor composition calculated from (2). A comparison of steady-state composition profiles obtained from the Aspen simulator and the wave model with the nominal parameter values are shown in Fig. 2. Satisfactory results were produced at the nominal operating point because the wave parameters were adjusted to compensate for modeling errors introduced by the wave model assumptions. Poor pre-

dictions were obtained at the other three steady states, thereby motivating the development of an on-line estimation strategy.

4.2. Measurement selection and estimator design

We performed off-line estimation of the wave model parameters for five steady states corresponding to feed flow rate changes of ± 5 kmol/h and ± 10 kmol/h from the nominal value. Although not shown here, the lower asymptotic limit y_{min} exhibited only small variations over this range of operating conditions. Therefore, y_{min} was fixed at zero and the wave position s, wave front slope γ and upper asymptotic limit y_{max} were treated as the estimated variables. The liquid composition on each equilibrium stage was considered as a candidate measurement, yielding a total of 41 possible measurement locations. All compositions were natural log transformed since the oxygen content in the upper part of the column is at ppm levels. Table 2 provides a comparison of the measurement rankings obtained with the proposed PCA based technique and the standard SVD method (Oisiovici and Cruz, 2001). Results are shown for five different steady states and an "averaged gain" case where the measurement selection methods were applied to an composite gain matrix obtained by element-by-element averaging of the gain matrices at the five steady states. The averaged gain case was intended to generate rankings that are appropriate over a range of operating conditions rather than a single steady-state.

The measurement rankings obtained with the PCA method are easily interpreted using the corresponding Aspen composition profiles. The following trends are observed: (1) the stage one composition was always selected due to its large gain when the compositions were log transformed; (2) the highest ranked measurements were located near the wave position (inflection point) because compositions in this range were very sensitive to small parameter changes; (3) adjacent stage compositions were not favored due to their high collinearities; and (4) stages located in highly pinched regions of the composition profile were not chosen because of their small gains. Similar trends were observed with SVD method. The two highest ranked measurements obtained with each selection method were identical,
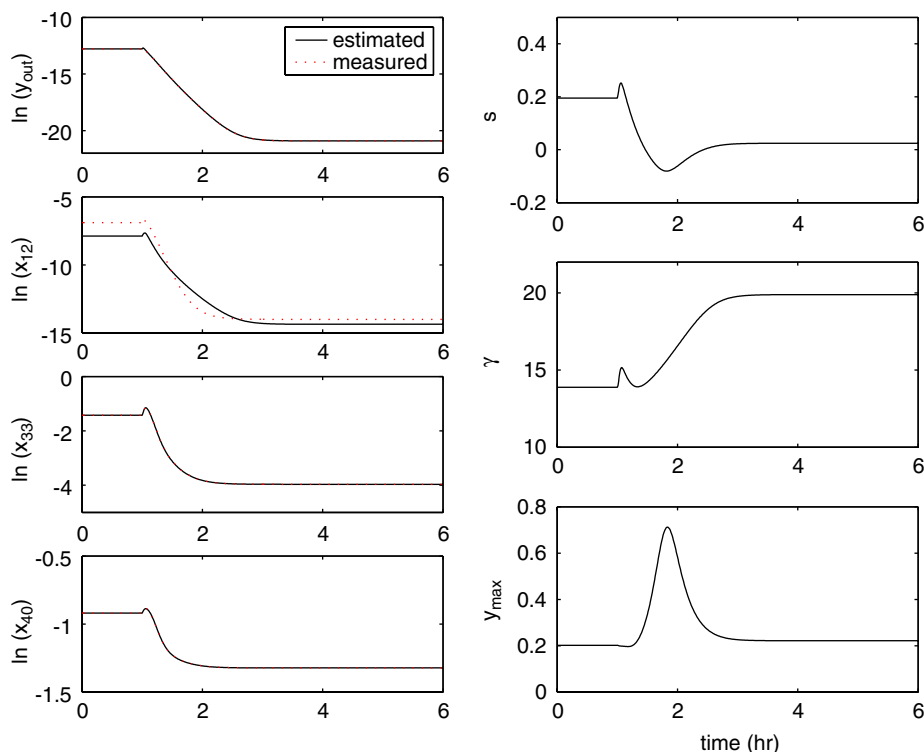
Fig. 3. Estimator performance for an increase in the air feed flow rate.

and only small differences were observed for the third measurement. However, SVD method is not capable of ranking more measurements than the number of estimated variables. Therefore, the proposed PCA method can be loosely viewed as an extension without this limitation on the number of ranked measurements. Below we show that this distinction is critically important when the number of on-line measurements must exceed the number of estimated variables to obtain satisfactory estimator performance.

Combined state and parameter estimation was performed with a discrete-time formulation of the first-order extended Kalman filter (EKF) (Gelb, 1974; Muske and Edgar, 1997). At each time step the nonlinear wave model was linearized at the previous estimates and the filter gain was evaluated using the discrete Riccati equation. We found that four measurements were needed to robustly estimate the three wave variables (s, γ, y_{max}) over a range of operating conditions. The fourth measurement was required to avoid observability problems resulting in estimator divergence when one measurement became located in a highly pinched region of the composition profile. The four measurements used were obtained directly from the PCA averaged gain entry in Table 2: the top stage vapor composition (y_{out}) and the liquid compositions on stages 12, 33 and 40. Because there are insufficient degrees of freedom to obtain bias free estimates of all four measurements, the EKF covariances were tuned to localize the bias to the intermediate stage composition x_{12}. Additional details about the EKF formulation and tuning are available in our previous publication (Bian et al., 2005).

4.3. Simulation results

Fig. 3 shows the performance of the EKF when the air feed flow rate was increased by 10 kmol/h at $t = 1$ h. The Aspen composition wave moved downward in the column because the positive change in the feed flow rate induced a reflux flow rate increase. The EKF produced rapid and unbiased tracking of y_{out}, x_{33} and x_{40}, while the x_{12} estimate was biased due to the EKF tuning used. Although achieved only temporarily, a negative estimate of the wave position s is physically meaningful when the inflection point of the composition profile moves outside the column. Due to end effects not captured by the wave model (Marquardt, 1986), the wave became sharper when the inflection point approached the bottom of the column. The EKF compensated for this unmodeled effect by increasing the estimate of the wave slope parameter γ. While the upper asymptotic limit y_{max} increased transiently, the initial and final steady-state values were very similar.

Fig. 4 shows composition profiles reconstructed from the EKF state and parameter estimates for the 10 kmol/h increase in the air feed flow rate. The symbols are Aspen values and the solid lines are EKF reconstructed profiles at the indicated times. The EKF provided excellent agreement with the Aspen profiles, particularly at the new steady-state. Reconstructed composition profiles for five different steady states are shown in Fig. 5. The EKF produced satisfactory agreement with each Aspen profile despite the large movement of the composition profile that occurred over this range of feed flow rates. Although not shown here, stable estimator performance could not be obtained with
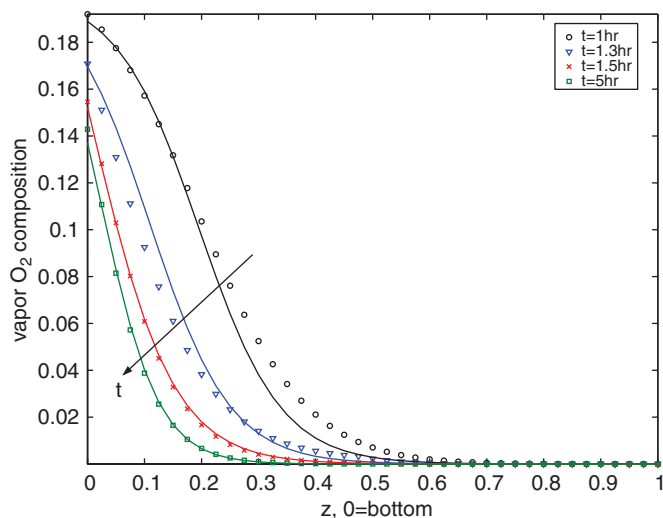
Fig. 4. Reconstructed dynamic composition profiles for an increase in the air feed flow rate.
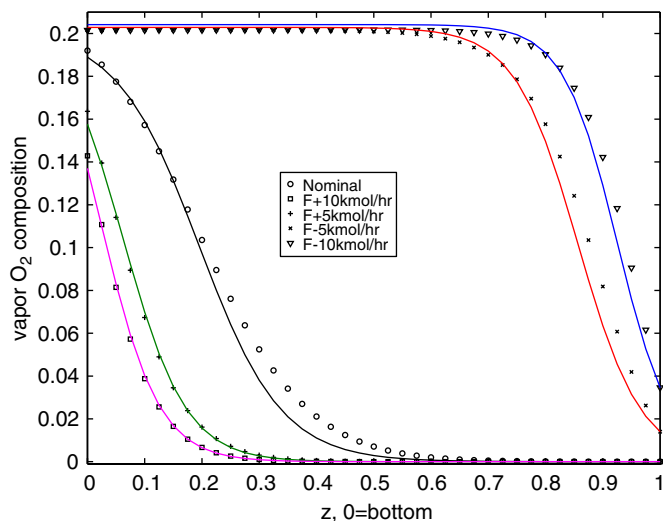
Fig. 5. Reconstructed steady-state composition profiles for the nitrogen purification column.

only three composition measurements due to the movement of the highly pinched region. A comparison of these results with the open-loop estimation results in Fig. 5 clearly demonstrates the value of on-line estimation with rationally selected measurement locations for this ultra high purity nitrogen purification column.

5. Benzene–toluene separation column

5.1. Model formulation

Now we consider the benzene–toluene separation column in the HDA process for benzene production (Douglas, 1988). The trayed column has a total of 22 equilibrium stages including the reboiler and a total condenser. A ternary mixture of benzene, toluene and trace amounts of diphenyl is introduced

at stage 13. The overhead product is purified benzene while the bottoms product is mainly toluene with residual benzene and a small amount of diphenyl. A dynamic simulation of the benzene–toluene column was constructed in Aspen dynamics and utilized as a surrogate plant in our simulation studies. The nominal operating conditions of the Aspen simulator are shown in Table 3. Two other steady states corresponding to feed flow rate changes of $\pm 10\%$ of the nominal value were also investigate to cover a reasonable range of column operating conditions.

Because the benzene–toluene column has both stripping and rectifying sections, two nonlinear waves were required to model the column dynamics. The dynamics of the feed stage, condenser and reboiler were neglected since their holdups were much smaller than the total holdup of each column section. Therefore, the two waves were connected through a steady-state composition balance on the feed stage. A pseudo-binary feed mixture was constructed with toluene and diphenyl lumped into a single component. Ideal vapor–liquid equilibrium was assumed with a constant relative volatility regressed from Aspen composition profile data. The complete wave model consisted of two nonlinear differential equations for the wave positions and 11 nonlinear algebraic equations for steady-state feed stage, reboiler and condenser balances and the vapor–liquid equilibrium relations. Nominal values of the two wave positions (s_r, s_s) and the six wave profile parameters $(\gamma_r, y_{\min,r}, y_{\max,r}, \gamma_s, y_{\min,s}, y_{\max,s})$ were regressed from the nominal Aspen composition profile. Fig. 6 shows open-loop composition profile predictions obtained with the nominal wave parameters for three different steady states. As expected, excellent agreement with the Aspen composition profile was obtained at the nominal operating point. Unsatisfactory agreement was obtained in the rectifying section for the $F + 10\%$ change and in the stripping section for the $F - 10\%$ change due to wave distortion caused by end effects and non-ideal column behavior.

5.2. Measurement selection and estimator design

Off-line estimation at the nominal, $F - 10\%$ and $F + 10\%$ steady states was used to determine the wave profile parameters included in the on-line estimation problem. The rectifying upper asymptotical limit $(y_{\max,r})$ and the stripping lower asymptotical limit $(y_{\min,s})$ exhibited very small variations between the three steady-states. Consequently, we fixed $y_{\min,s} = 0$ and $y_{\max,r} = 1$, and treated the two wave positions (s_r, s_s) and the four remaining parameters $(\gamma_r, y_{\min,r}, \gamma_s, y_{\max,s})$ as estimated variables. The vapor composition of each stage and the reboiler liquid composition were considered as candidate measurements. A comparison of the measurement rankings obtained with the proposed PCA based technique and the SVD method are shown in Table 4 for the same steady states and the averaged gain case. The two methods produced identical rankings of the first three measurements, but different rankings of the next three measurements due to algorithmic differences.

Table 3
Nominal operating conditions for benzene–toluene column

Variable	Symbol (units)	Value
Feed flow rate	F (kmol/h)	134.7
Feed vapor fraction	q (kmol/kmol)	0
Feed benzene composition	z_f (kmol/kmol)	0.532
Top stage vapor composition	y_{out} (kmol/kmol)	0.9934
Reboiler liquid composition	x_B (kmol/kmol)	0.0121
Average liquid holdup on each stage (rectifying section)	$n_{l,r}$ (kmol)	1.038
Average vapor holdup on each stage (rectifying section)	$n_{v,r}$ (kmol)	0.0407
Average liquid holdup on each stage (striping section)	$n_{l,s}$ (kmol)	1.058
Average vapor holdup on each stage (striping section)	$n_{v,s}$ (kmol)	0.0410
Bottom product flow rate	B (kmol/h)	63.35
Overhead product flow rate	D (kmol/h)	71.37
Reflux flow rate	L (kmol/h)	128.4

Fig. 6. Open-loop simulation results for the benzene–toluene column.

Table 4
Measurement selection results for the benzene–toluene column

Method	Steady-state	1st	2nd	3rd	4th	5th	6th	7th	8th
PCA	Nominal	17	10	14	12	20	6	15	16
PCA	$F - 10$ kmol/h	15	4	12	14	18	1	7	5
PCA	$F + 10$ kmol/h	14	20	11	12	22	18	21	9
PCA	Averaged gain	16	12	14	4	21	8	20	1
SVD	Nominal	17	10	14	12	18	8	N/A	N/A
SVD	$F - 10$ kmol/h	15	4	12	14	1	19	N/A	N/A
SVD	$F + 10$ kmol/h	14	20	11	12	18	22	N/A	N/A
SVD	Averaged gain	16	12	14	22	4	9	N/A	N/A

Table 5
Measurement selection results for the benzene–toluene column with stage one fixed as the highest ranked measurement location

Steady-state	1st	2nd	3rd	4th	5th	6th	7th	8th
Nominal	1	17	14	12	9	20	15	16
$F - 10$ kmol/h	1	15	12	14	5	18	7	3
$F + 10$ kmol/h	1	20	14	12	21	10	18	22
Averaged gain	1	16	12	14	21	9	22	19

An important advantage of the proposed method is that existing measurements can be preselected without modifying the ranking algorithm. The overhead vapor composition of the benzene–toluene column is typically measured to provide a direct indication of the benzene product purity. Table 5 shows the results obtained when the overhead vapor composition was fixed to be the highest ranked measurement and the remaining measurements were ranked as usual. As expected different rankings of the remaining measurements were obtained compared to the regular case in Table 4. Unlike the nitrogen purification column considered earlier, robust estimation over a reasonable range of feed flow rates was achieved with the same number of measurements and estimated variables because the composition profile was not highly pinched. The EKF was designed to estimate the two wave positions (s_r, s_s) and the four wave parameters $(\gamma_r, y_{\min,r}, \gamma_s, y_{\max,s})$ using the six highest ranked measurements for the PCA average gain entry in Table 4 or 5 depending on the case being considered. For both cases the EKF was readily tuned to provide stable and bias free tracking of Aspen composition profiles.

5.3. Simulation results

Fig. 7 shows EKF performance when the six estimates were generated from on-line measurements of the stages 4, 8, 12, 14, 16 and 21 vapor compositions as listed in Table 4 for the PCA average gain case. The column was subjected to a 10% feed flow rate increase at $t = 1$ h that caused the Aspen rectifying and stripping composition profiles to move towards the bottom of their respective sections. The EKF produced excellent tracking of the six measurements while generating reasonable state and parameter estimates consistent with a slight sharpening of the stripping section wave due to end effects. While smoother parameter estimates could be obtained by retuning the EKF covariance matrices, only slight improvements were possible due to strong correlations between parameter effects. For example γ_s and $y_{\max,s}$ have very similar effects on the upper part of the stripping section and the entire rectifying section. Consequently, the parameter
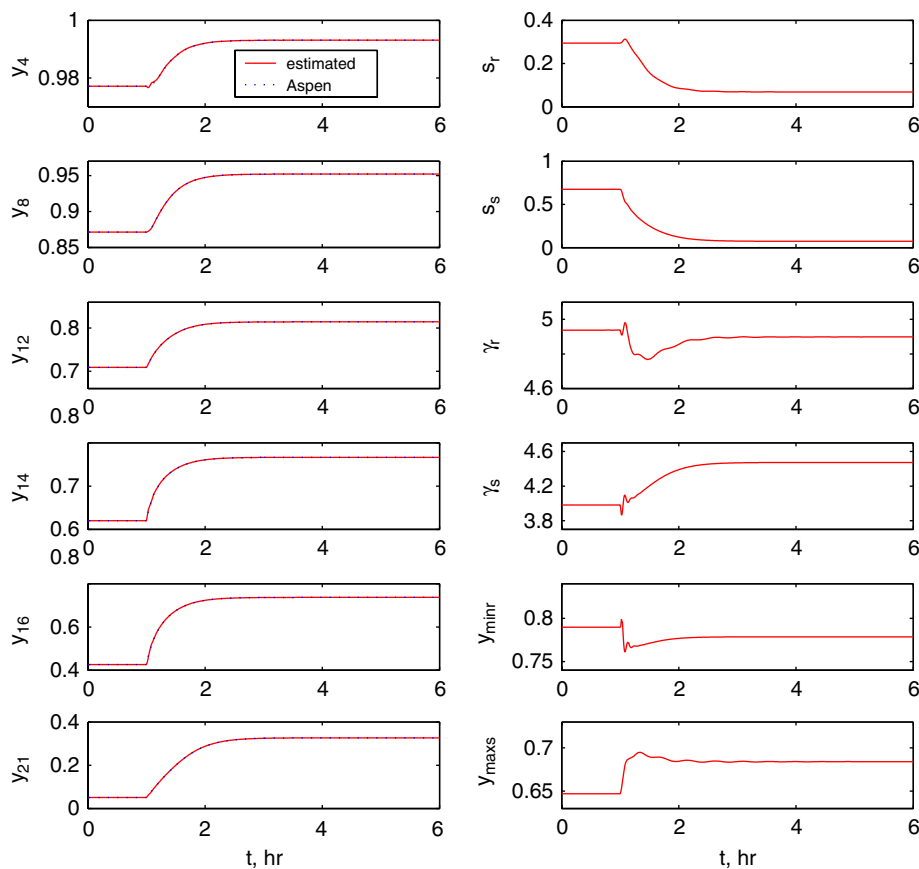
Fig. 7. Estimator performance for an increase in the feed flow rate.
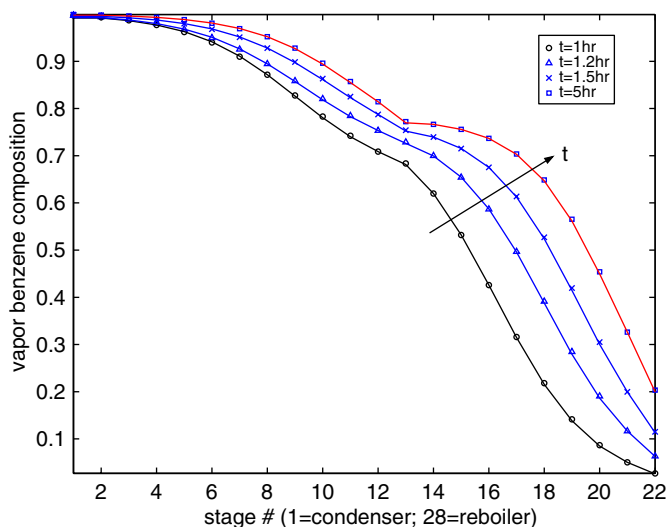
Fig. 8. Reconstructed dynamic composition profiles for a feed flow rate increase to the benzene–toluene column.
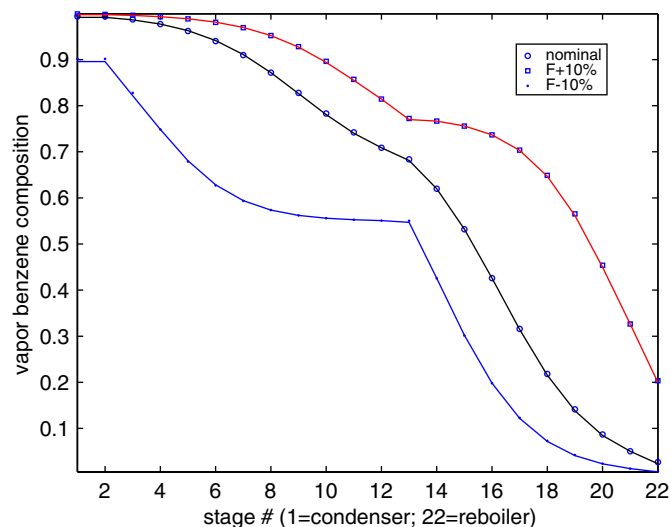
Fig. 9. Reconstructed steady-state profiles of the benzene–toluene column.

estimates required to eliminate estimation bias were not unique. We suspect that this non-uniqueness problem was at least partially responsible for the non-smooth parameter estimates. Transient composition profiles reconstructed from the EKF state and parameter estimates are shown as solid lines in Fig. 8. Corresponding steady-state estimation results are shown in Fig. 9 for three different operating points. The EKF produced excellent dynamic and steady-state agreement with the Aspen composition values (symbols) in both column sections.
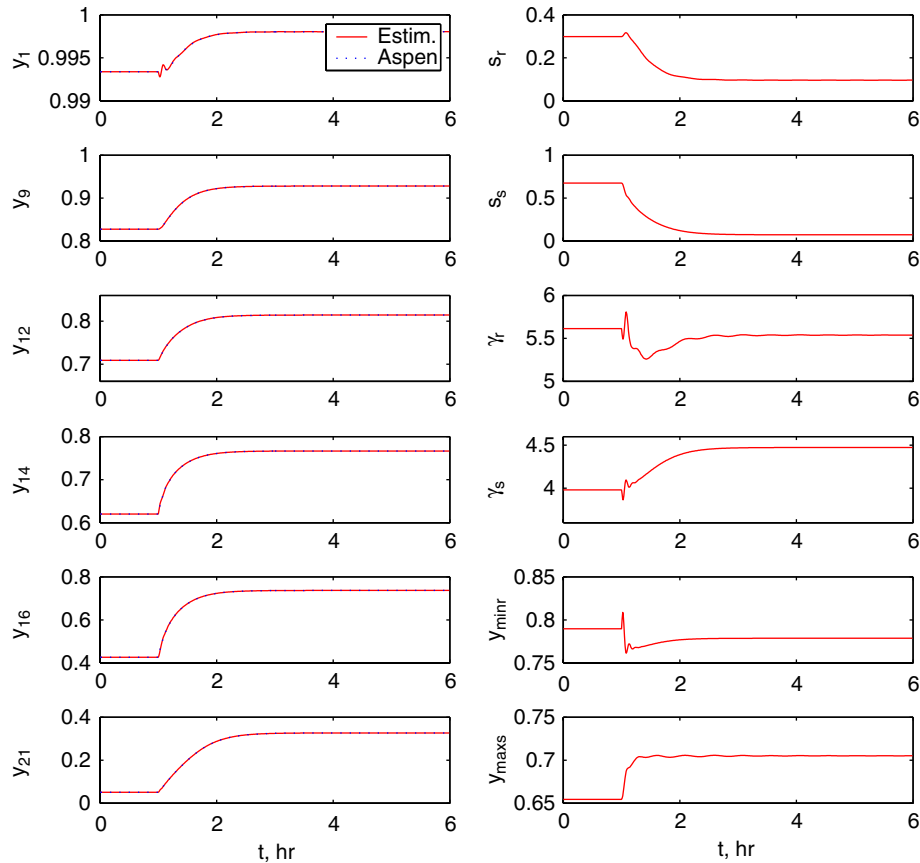
Fig. 10. Estimator performance when the overhead composition is a preselected measurement.

Next EKF performance was evaluated when the six estimates were generated from the available overhead composition measurement and the next five highest ranked composition measurements (stages 9, 15, 18, 25 and 27) listed for the average gain entry in Table 5. Fig. 10 shows predicted compositions at the six measurement locations along with the state and parameter estimates for the same feed flow rate increase considered above. Reconstructed steady-state composition profiles are shown in Fig. 11. Despite inclusion of the stage 1 composition previously considered to be a poor measurement (see Table 4), EKF performance was only slightly degraded as compared to the regular case in Fig. 7. These simulation results demonstrate that the proposed measurement selection procedure is sufficiently flexible for industrial applications where existing measurements must be combined with new measurements to achieve successful on-line estimation.

A fundamental limitation of nonlinear wave models is observed when the inflection point of the composition profile moves far beyond a physical boundary of the column section. The wave position s can assume a value significantly below zero when the profile moves sharply downward and a value significantly above unity when the profile moves sharply upward. Such composition profiles are inherently difficult to reconstruct with wave models because all candidate measurements provide information only for a limited portion of the profile located in-
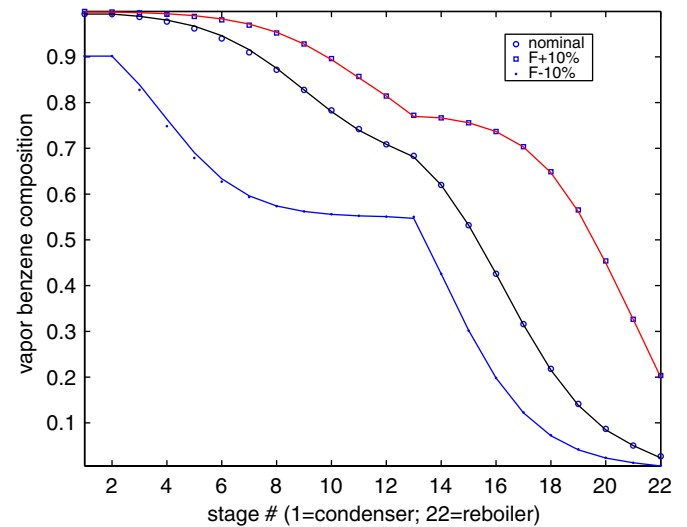
Fig. 11. Reconstructed steady-state profiles when the overhead composition is a preselected measurement.

side the physical section boundaries. To illustrate this problem we considered a modified version of the benzene–toluene column with three additional theoretical stages added to both the rectifying and stripping sections. This change produced a much

Table 6
Measurement selection results for the modified benzene–toluene column with six estimated parameters

Steady-states	1st	2nd	3rd	4th	5th	6th	7th	8th
Nominal	1	25	29	17	15	23	26	18
$F - 10\,\text{kmol/h}$	1	29	21	16	17	6	26	3
$F + 10\,\text{kmol/h}$	1	29	25	15	26	11	23	16
Averaged gain	1	25	27	18	15	9	26	23

Table 7
Measurement selection results for the modified benzene–toluene column with five estimated parameters

Steady-state	1st	2nd	3rd	4th	5th	6th	7th	8th
Nominal	1	25	29	17	15	23	26	18
$F - 10\,\text{kmol/h}$	1	29	21	16	18	10	26	6
$F + 10\,\text{kmol/h}$	1	29	25	15	27	23	16	11
Averaged gain	1	25	27	18	14	23	20	26

higher purity separation with a benzene product composition of 0.9997 and a bottoms product composition of 0.0065. Off-line estimation studies showed that the wave slopes γ_r and γ_s varied only slightly for $\pm 10\%$ feed flow rates changes. Therefore, we fixed the wave slopes at their nominal values $\gamma_r = 6.21$ and $\gamma_s = 5.41$ and treated the two wave positions (s_r, s_s) and the four asymptotic limits $(y_{\min,r}, y_{\max,r}, y_{\min,s}, y_{\max,s})$ as estimated variables.

Table 6 shows the measurement rankings obtained with the proposed algorithm for this new case. The first six measurements for the average gain entry were used to generate EKF estimates of the wave positions and asymptotic limit parameters. Fig. 12 shows EKF performance for a 10% decrease in the feed flow rate. While the measured compositions were effectively tracked, the wave position s_r and upper asymptotic

limit $y_{\max,r}$ in the rectifying section simultaneously diverged due to an observability problem caused by the wave profile moving out the top of the rectifying section. EKF divergence was attributable to an inherent limitation of the wave model rather than a shortcoming of the proposed measurement selection procedure. We were not able to find any combination of on-line measurements that eliminated the divergence problem.

The only recourse was to formulate a different estimation problem by selecting a new set of estimated parameters. We fixed the diverging parameter $y_{\max,r} = 1$ and estimated the remaining three asymptotic limit parameters with the first five measurements listed for the average gain entry in Table 7. Fig. 13 shows the performance of the modified EKF for a 10% decrease in the feed flow rate. Removal of the unobservable parameter $y_{\max,r}$ produced stable estimator performance as well
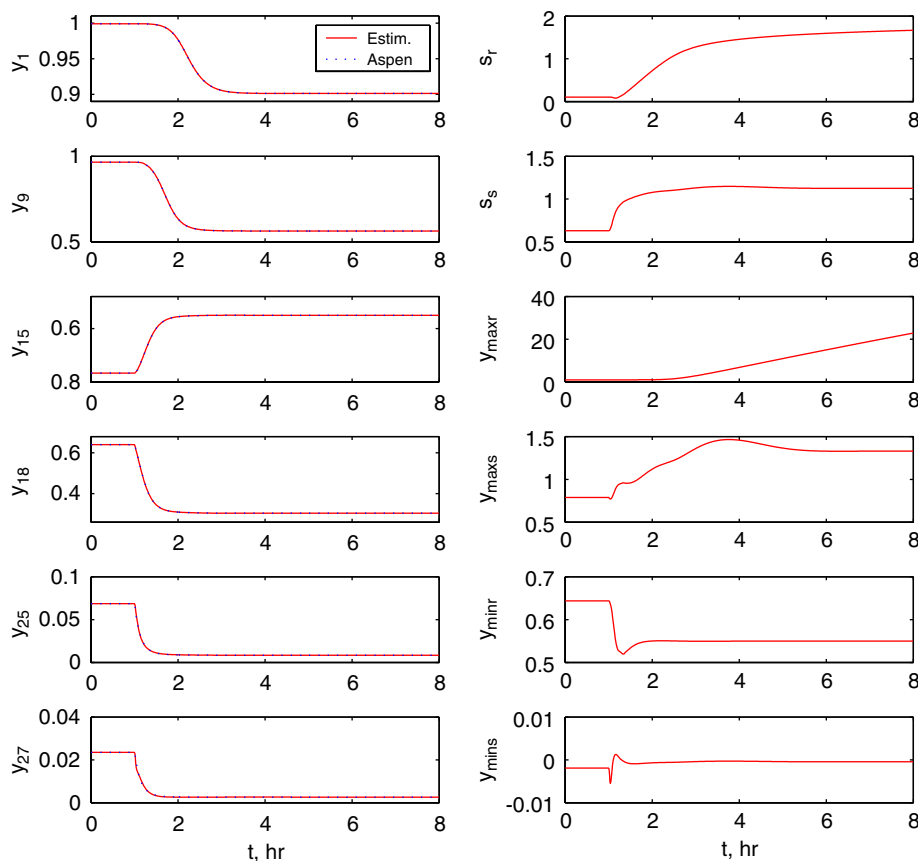
Fig. 12. Estimator performance for the modified benzene–toluene column with six estimated variables.
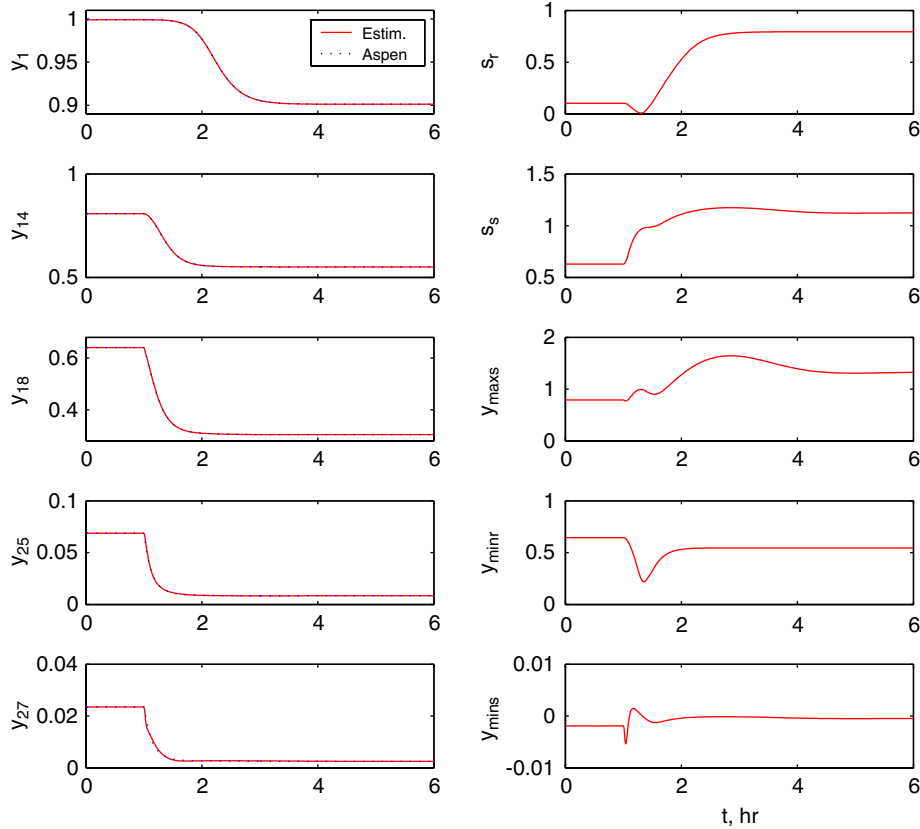
Fig. 13. Estimator performance for the modified benzene–toluene column with five estimated variables.
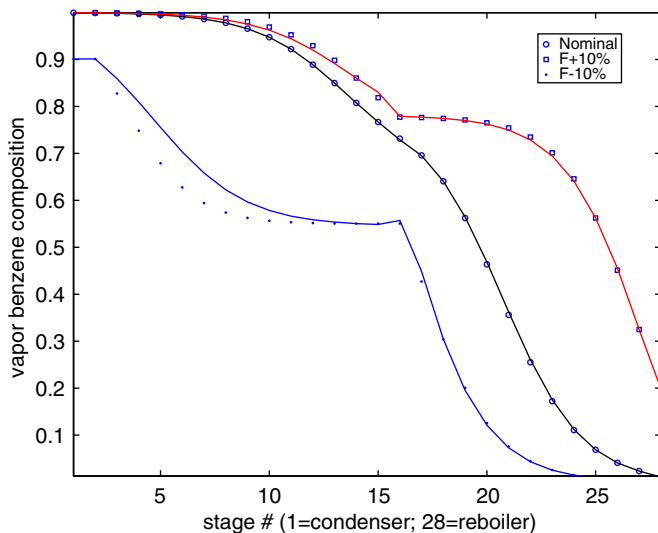
Fig. 14. Reconstructed steady-state profiles for the modified benzene–toluene column with five estimated variables.

6. Summary and conclusions

A general method for selecting candidate measurements for on-line state and parameter estimation was presented. While sharing similarities with existing techniques based on singular value decomposition, the proposed method offers several important advantages including the ability to: (1) rank more measurements than the number of estimated variables; and (2) allow the inclusion of existing plant measurements. We focused on the selection of stage composition measurements for on-line estimation of nonlinear wave models that capture the essential dynamics of high purity distillation columns. The measurement selection procedure was successfully utilized to construct combined state/parameter estimators for a nitrogen purification column and a benzene–toluene separation column using the extended Kalman filtering approach. The ultra high purity nitrogen column required one more measurement than the number of estimated variables to ensure stable EKF performance due to the presence of highly pinched composition profiles. Excellent EKF performance was obtained for the benzene–toluene column when the product purity requirements were modest. A modified benzene–toluene column designed to produce higher purity products caused EKF divergence due to an inherent observability problem associated with wave models. A heuristic redesign of the estimator was performed to eliminate the observability problem and generate stable EKF estimates. The simulation results presented suggest that the proposed

as unbiased tracking of the measured compositions. The reconstructed steady-state composition profiles shown in Fig. 14 were generally satisfactory with the possible exception of the rectifying section predictions for the 10% feed flow rate decrease.

method is sufficiently flexible to address a wide range of practical measurement selection problems.

Acknowledgements

References

Bagajewicz, M., 1997. Optimal sensor location in process plants. American Institute of Chemical Engineers Journal 43, 2300–2306.

Balasubramhanya, L.S., Doyle, F.J., 1997. Nonlinear control of a high-purity distillation column using a traveling-wave model. American Institute of Chemical Engineers Journal 43, 703–714.

Bian, S., Henson, M.A., Belanger, P., Megan, L., 2005. Nonlinear state estimation and model predictive control of nitrogen purification columns. Industrial and Engineering Chemistry Research 44, 153–167.

Biegler, L.T., Cervantes, A.M., Wachter, A., 2002. Advances in simultaneous strategies for dynamic process optimization. Chemical Engineering Science 57, 575–593.

Chmielewski, D.J., Palmer, T., Manousiouthakis, V., 2002. On the theory of optimal sensor placement. American Institute of Chemical Engineers Journal 48, 1001–1012.

Douglas, J.M., 1988. Conceptual Design of Chemical Processes. McGraw-Hill, NY.

Dunteman, G.H., 1989. Principal Components Analysis. Sage, Newbury Park, CA.

Gelb, A., 1974. Applied Optimal Estimation. MIT Press, Cambridge, MA.

Gilles, E.D., Retzbach, B., 1983. Reduced models and control of distillation columns with sharp temperature profiles. IEEE Transactions on Automatic Control 28, 628–630.

Henson, M.A., 1998. Nonlinear model predictive control: current status and future directions. Computers and Chemical Engineering 23, 187–202.

Hwang, Y.-L., 1987. Dynamics of continuous countercurrent mass transfer processes—I. Single-component linear systems. Chemical Engineering Science 42, 105–123.

Hwang, Y.-L., Helfferich, F.G., 1988. Dynamics of continuous countercurrent mass transfer processes—II. Single-component systems with nonlinear equilibria. Chemical Engineering Science 43, 1099–1114.

Isalski, W.H., 1989. Separation of Gases. Oxford Press, NY.

Li, R., Henson, M.A., Kurtz, M.J., 2004. Selection of model parameters for off-line parameter estimation. IEEE Transactions on Control Systems Technology 12, 402–412.

Luyben, W.L., 1972. Profile position control of distillation columns with sharp temperature profiles. American Institute of Chemical Engineers Journal 18, 238.

Luyben, W.L., 1973. Process Modeling Simulation and Control for Chemical Engineers. McGraw-Hill, New York, NY.

Marquardt, W., 1986. Nonlinear model reduction for binary distillation. In: Proceedings of IFAC Control of Distillation Columns and Chemical Reactors, Bournemouth, UK, pp. 123–128.

Mayne, D.Q., Rawlings, J.B., Rao, C.V., Scokaert, P.O.M., 2000. Constrained model predictive control: stability and optimality. Automatica 36, 789–814.

Meadows, E.S., Rawlings, J.B., 1997. Model predictive control. In: Henson, M.A., Seborg, D.E. (Eds.), Nonlinear Process Control. Prentice-Hall, Englewood Cliffs, NJ, pp. 233–310 (Chapter 5).

Muske, K.R., Edgar, T.F., 1997. Nonlinear state estimation. In: Henson, M.A., Seborg, D.E. (Eds.), Nonlinear Process Control. Prentice-Hall, Englewood Cliffs, NJ, pp. 311–370 (Chapter 6).

Muske, K.R., Georgakis, C., 2003. Optimal measurement system design for chemical processes. American Institute of Chemical Engineers Journal 49, 1488–1494.

Nagy, Z., Findeisen, R., Diehl, M., Allgower, F., Bock, H.G., Agachi, S., Schloder, J.P., Leineweber, D., 2000. Real-time feasibility of nonlinear predictive control for large scale processes—a case study. In: Proceedings of American Control Conference, Chicago, IL, pp. 4249–4254.

Oisiovici, R.M., Cruz, S.L., 2001. Inferential control of high-purity multicomponent batch distillation columns using an extended Kalman filter. Industrial and Engineering Chemistry Research 40, 2628–2639.

Rehm, A., Allgower, F., 1996. Nonlinear H_∞ control of a high purity distillation column. In: UKACC International Conference on Control'96, Exeter, UK, 1996, pp. 1178–1183.

Zhu, G.-Y., Henson, M.A., Megan, L., 2001. Low-order dynamic modeling of cryogenic distillation columns based on nonlinear wave phenomenon. Separation and Purification Technology 24, 467–487.